ISSN 1618-2642, Volume 397, Number 4

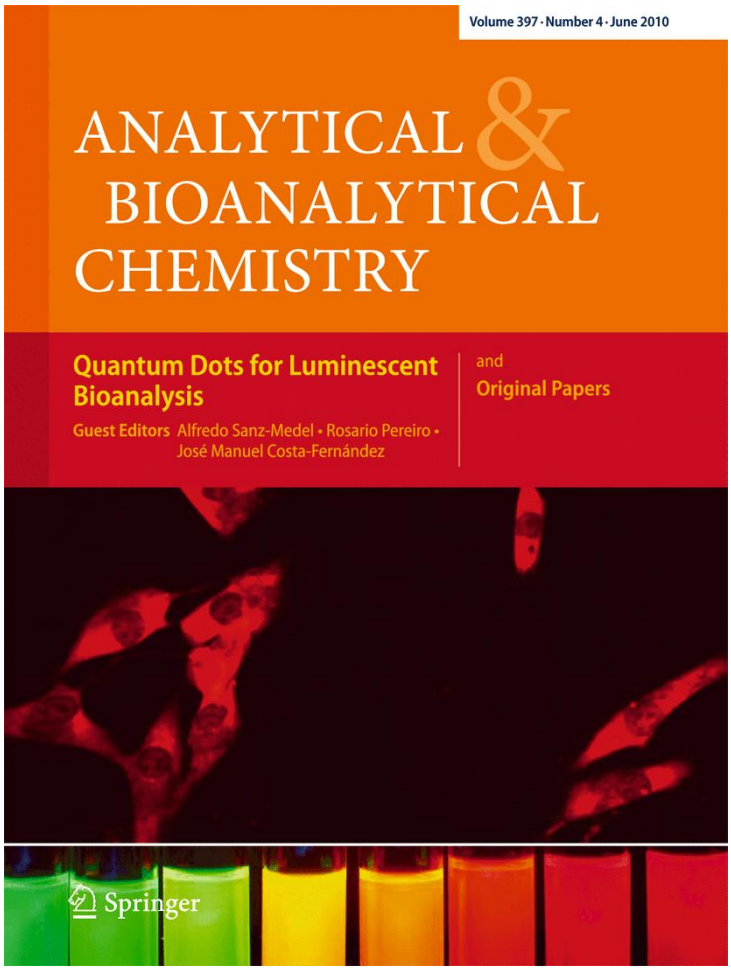

Anal Bioanal Chem (2010) 397:1511–1519
DOI 10.1007/s00216-010-3690-z

ORIGINAL PAPER

Detection of chemical agents in the atmosphere by open-path FT-IR spectroscopy under conditions of background interference: I. High-frequency flashes

Limin Shao · Christopher W. Roske · Peter R. Griffiths

Received: 7 October 2009 / Revised: 22 February 2010 / Accepted: 25 March 2010 / Published online: 18 April 2010

Abstract Open-path FT-IR spectra were measured while fireworks were emitting smoke and incandescent particles into the infrared beam. These conditions were designed to simulate the appearance of smoke and explosions in a battlefield. Diethyl ether was used to simulate the vapor-phase spectra of G agents such as sarin. The measured interferograms were corrected by a high-pass filter and were rejected when interfering features were of such high frequency that they could not be removed by application of this filter. The concentration of diethyl ether was calculated correctly by partial least squares regression in the absence of fireworks but significant errors were encountered when the spectra of the oxide particles were not included in the calibration set. Target factor analysis allowed the presence of the analyte to be detected even when the incandescent particles were present in the beam.

Keywords Open-path FT-IR spectrometry · Battlefield clutter · G agents · Fireworks · PLS regression · Target factor analysis

Introduction

The detection of chemical warfare agents released by missile strikes is clearly an important component of modern warfare. Any instrumental technique for detecting chemical agents in the atmosphere near battlefields should be rapid (measurements in a few seconds), selective (a low number of false positives and false negatives), sensitive (parts-per-billion [ppb] sensitivity), and subject to minimal interference in the presence of explosives and other battlefield events. Open-path Fourier transform infrared (OP/FT-IR) spectroscopy fulfills the first three of these criteria [1-4]. Measurements can be made in times between 1 s and 1 min, depending on the resolution and sensitivity desired. The spectra of the G agents, e.g., Sarin, Soman, and Tabun, have at least one strong absorption band in the 10-μm atmospheric window (between about 800 and 1250 cm^{-1}). The high absorptivity of these bands leads to detection limits of less than 10 ppb provided that the pathlength is at least 100 m. Even though the G agents are all phosphonate esters, their infrared spectra are sufficiently different to allow them to be distinguished with high confidence [5].

As a consequence of these properties, both active and passive OP/FT-IR spectroscopy are being investigated by the US military as a way to detect chemical warfare agents, including detection under battlefield conditions. This type of measurement may be severely hindered if any event takes place that distorts the interferogram. If this is the case, the measured spectra show artifacts that prevent the successful application of the type of algorithms used to process the data in calmer, more pristine atmospheres. We have been investigating the feasibility of applying partial least squares regression (PLS) and target factor analysis (TFA) to spectra that have been measured under conditions that severely distort interferograms in order to detect the onset of the appearance of chemical agents in the atmosphere.

This work was initiated when we were involved in a project sponsored by the US Department of Agriculture to measure the concentrations of molecules in the atmosphere

L. Shao
Department of Chemistry,
University of Science and Technology of China,
Hefei, Anhui 230026, China

C. W. Roske · P. R. Griffiths (✉)
Department of Chemistry, University of Idaho,
Moscow, ID 83844-2343, USA
e-mail: pgriff@uidaho.edu

around cattle and hog farms in Southern Idaho [3, 6, 7]. We observed frequent interference during these measurements and it was not unusual to find the baseline of the interferogram distorted because a bird or a vehicle had passed through the beam during data acquisition. To allow most of these measurements to either yield accurate quantitative data or to be rejected, we developed criteria to which each interferogram was subjected [7].

Three reasonable assumptions were made: (a) the first interferogram that is measured immediately after measurements are initiated is deemed to be normal; (b) the signal is proportional to the maximum value of the *i*th interferogram, H_i; and (c) the noise or the presence of some type of abnormality may be estimated by calculating the standard deviation of the data over the first quarter of points in the interferogram before the centerburst or the last quarter of the points after the centerburst, $STD_{1/4}$. Although these points also contain real spectral information due to narrow lines in the rotation–vibration spectrum of atmospheric water vapor, the noise level of "bad" scans or some abnormally intense data points well away from the centerburst usually exceeds the signal in the wings of the interferogram.

To develop criteria for which "bad" interferograms can be rejected, a *noise level index* for the *i*th interferogram (NLI_i) is calculated as

$$NLI_i = \frac{STD_{1/4,i} H_1}{STD_{1/4,1} H_i} \quad (1)$$

where the subscript 1 refer to the first interferogram measured in a given set. Interferograms are rejected if NLI_i is significantly greater than 1; for our work, an interferogram is rejected if $NLI_i > 1.3$. In the measurements near agricultural facilities, this algorithm was found to be very successful, provided that the signal in the interferogram that corresponded to wavenumbers below the cut-off of the mercury cadmium telluride (MCT) detector, $\tilde{\nu}_{min}$, was filtered out. To this end, each interferogram was treated by a high-pass filter that rejected all information below a frequency, f_{min}, equal to $\{\tilde{\nu}_{min} f_{HeNe} / \tilde{\nu}_{HeNe}\}$. For our instrument, $\tilde{\nu}_{min} = 700\,cm^{-1}$, f_{HeNe}=20 kHz, and $\tilde{\nu}_{HeNe} = 15,800\,cm^{-1}$, so that f_{min} is a little above 850 Hz.

For the results reported in this paper, we used this algorithm when the frequency of the interference was both above and below 850 Hz so that interferograms with only low-frequency interference were corrected and retained while those with high-frequency interference were rejected. To create the interference, we ignited several fireworks with several different characteristics in the beam of an OP/FT-IR spectrometer while attempting to detect a low concentration of diethyl ether. Diethyl ether was selected as the probe because of its similar spectral characteristics to sarin, see Fig. 1. Since much of the spectrum could not be observed because of absorption by water vapor and carbon dioxide, only the spectral region between 1,250 and 888 cm^{-1} was used.

The measurements were made on the evening of July 8, 2008. During the 75-min duration of this experiment, 15 fireworks were ignited; each firework was held immediately below the infrared beam and emitted a colored smoke and a stream of incandescent particles into the path of the infrared beam. In some cases, these hot particles simply streamed through the IR beam with minimal change, so that the frequency of the interference was below 850 Hz. Others emitted particles that rapidly ignited ("crackled") as they passed through the beam. The signal from these fireworks had a very-high-frequency component that was picked up by the spectrometer's MCT detector, giving rise to quite intense spikes on the interferogram. If the frequency was less than 600 Hz, the effect on the interferogram was compensated by application of a high-pass filter. When the interference had a component with a frequency greater than 1 kHz, the effect on the interferogram could not be compensated and the interferogram was rejected.

Experimental

All spectra were measured in the monostatic mode at a resolution of 4 cm^{-1} with a Bomem OP/FT-IR spectrometer equipped with a Globar® source and an MB-100 interferometer. The 4-cm diameter beam from the interferometer was passed onto a beamsplitter from which the transmitted light was passed to a telescope where it was expanded to a diameter of about 22 cm (the reflected light was passed to a blackened sheet where it was totally absorbed [8]). The collimated beam that emerged from the telescope passed through a 27-m path to a cube-corner array retroreflector that reflected the beam back through the path to the telescope, where it was reconfigured to a diameter of 4 cm and passed onto the beamsplitter. The transmitted beam was passed to a paraboloidal mirror that focused it onto a photoconductive MCT detector. Each output spectrum resulted from co-adding four interferograms and apodization with the Norton–Beer "medium" function. All spectra were corrected for the non-linear response of the MCT detector by the algorithm that we described recently [9]. The spectra were not baseline-corrected.

Before the start of the measurement sequence, a short-path background spectrum was measured with the retroreflector held within 1 m of the telescope. Each single-beam spectrum in the measurement sequence was ratioed against this spectrum and converted to absorbance. In this way, the instrument response function was compensated but lines in the vibration–rotation spectrum of atmospheric water vapor below 1,250 cm^{-1} were still present in the spectrum.

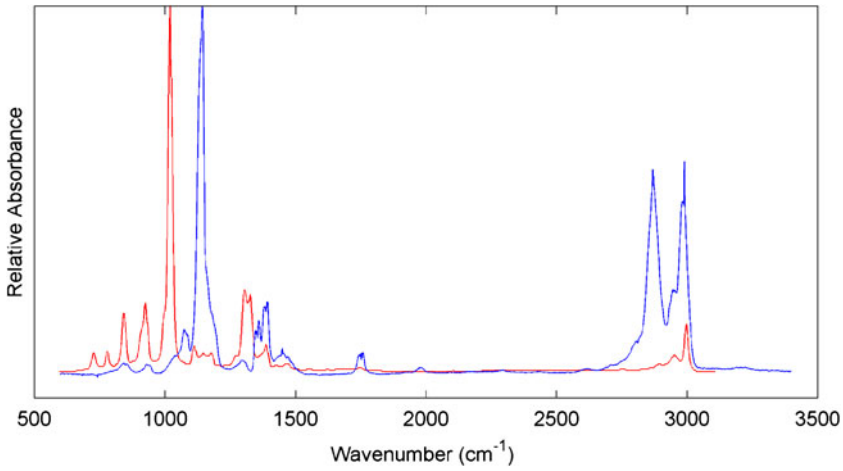

Fig. 1 Vapor-phase infrared reference spectra of diethyl ether (*blue*) and sarin (*red*); the spectra were normalized to fill the ordinate scale

A small volume of (liquid) diethyl ether was held in a Petri dish mounted half way between the instrument's telescope and retorereflector. A light westerly breeze was blowing when these measurements were being taken. To ensure that the ether that evaporated from the Petri dish did not remain in the path of the infrared beam for long, the beam was set up in a north–south configuration so that the analyte was quickly blown from the beam path.

Results and discussion

Measurements

The sequence of events is summarized in Fig. 2. The bottom bar shows when the Petri dish containing diethyl ether was mounted under the IR beam. The times when a significant concentration of ether should have been in the beam are shown in red at the bottom of this plot and the times when the Petri dish was removed, so that the ether concentration should be zero, are shown in green. The times when the fireworks were going off are shown as the red rectangles immediately above this bar.

Eight hundred nineteen spectra were measured sequentially in a total time of 75 min. The Petri dish was filled with diethyl ether for the first time at measurement 105 and refilled at 253. The Petri dish was removed at 310 and returned at 461. The diethyl ether in the Petri dish was ignited at 674 and the flame extinguished when all the ether had burned at 706. The Petri dish was refilled at 751 and remained until the end of the experiment. Of the 819 spectra that were measured, 42 were rejected because of the high-frequency interference.

A contour plot of all spectra that were not rejected is also shown in Fig. 2. The wavenumber of the strongest band in the spectrum of diethyl ether is indicated by the black arrow. From the intensity variations in the spectrum around 1,140 cm^{-1}, it can be seen that the concentration of the ether varied considerably during this sequence of measurements. It can also be seen that the material emitted by the

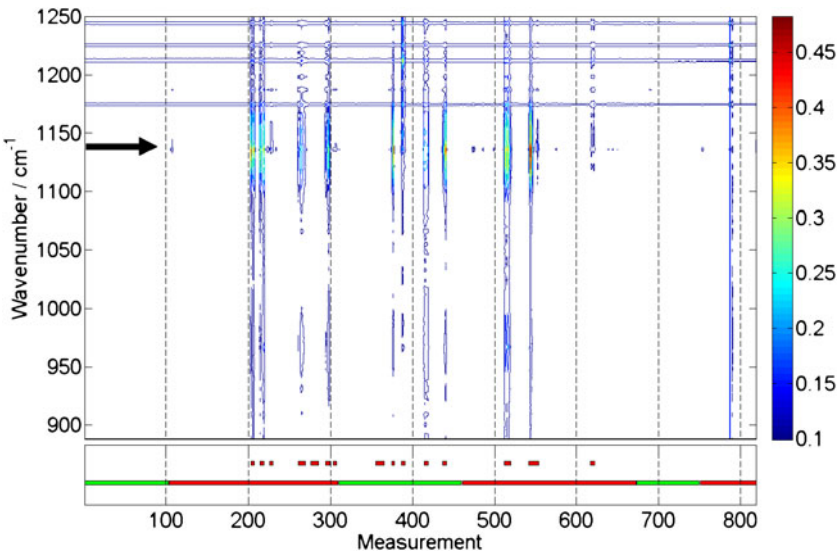

Fig. 2 Contour plot of 777 OP/FT-IR absorbance spectra from 1,250 to 888 cm^{-1}. Those absorbance spectra are arranged in order of time. The *lower bar* indicates the times when diethyl ether was present (*red*) or absent (*green*) in the beam. The *red rectangles above this bar* indicate the times when fireworks were emitting sparks and smoke into the beam

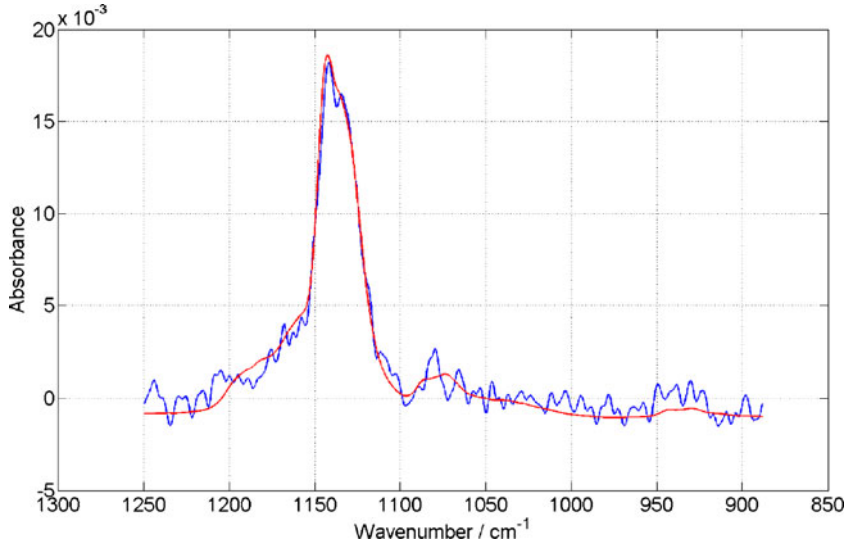

Fig. 3 The difference spectrum between spectra #105 and #104 (*blue*). The reference of spectrum of diethyl ether with a path-integrated concentration of 14 ppm m (*red*)

fireworks (which, from its spectral characteristics, appeared to be a mixture of metal oxides) gave rise to strong, broad absorption in the region around 1,140 cm^{-1}, entirely overlapping the strongest band in the spectrum of diethyl ether. A careful investigation of the spectra showed that the material emitted by the fireworks, while having similar spectra, was not always the same. The spectrum of diethyl ether measured right as the Petri dish was being filled with diethyl ether is shown in Fig. 3. Comparison with the reference spectrum of diethyl ether shows that the path-integrated concentration was 14 ppm m.

A fairly short path (27 m between the telescope and the retroreflector) was used for these measurements as the analyte and the fireworks were located in a short region about mid-way between the telescope and the retroreflector and any further increase in the pathlength would not have intensified the ether spectrum. The fireworks were located about 10 m from the retroreflector. Even though only a very small fraction of the radiation emitted by the fireworks was picked up by the telescope and retroreflector, it was enough to cause significant interference at the detector. Several different types of fireworks were used. Some, such as the

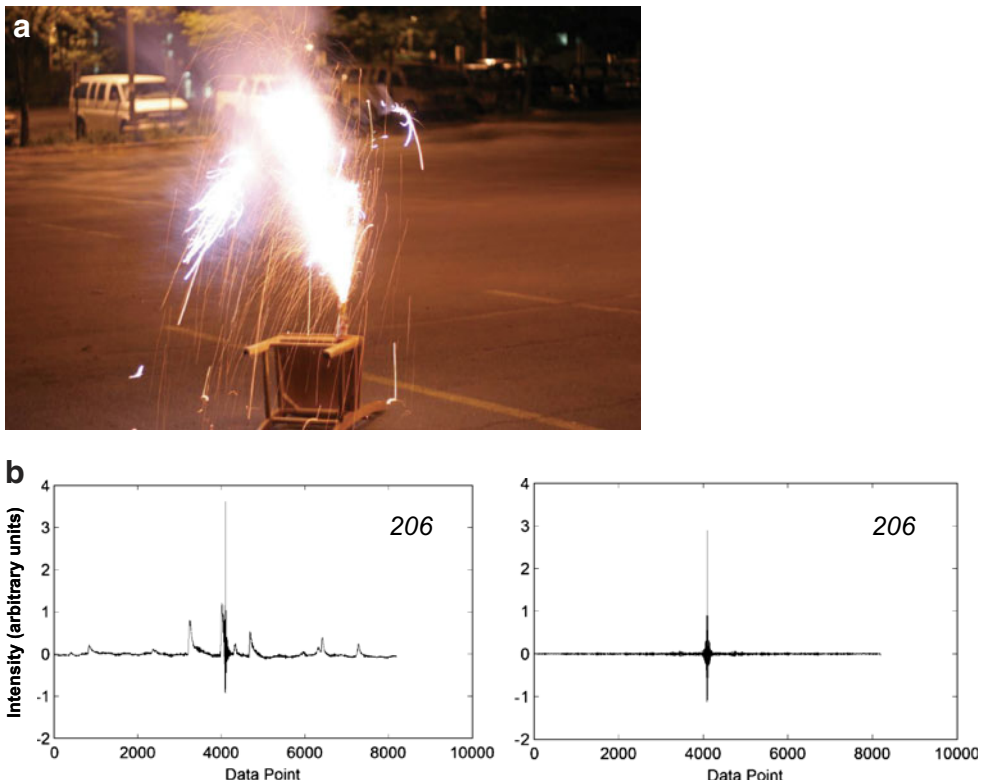

Fig. 4 **a** Firework during the acquisition of spectrum 206. **b** Interferogram measured during ignition of the firework shown in **a** (*left*) as measured and (*right*) after application of the high-pass filter. All interferograms measured during ignition of this firework were passed by the rejection criterion

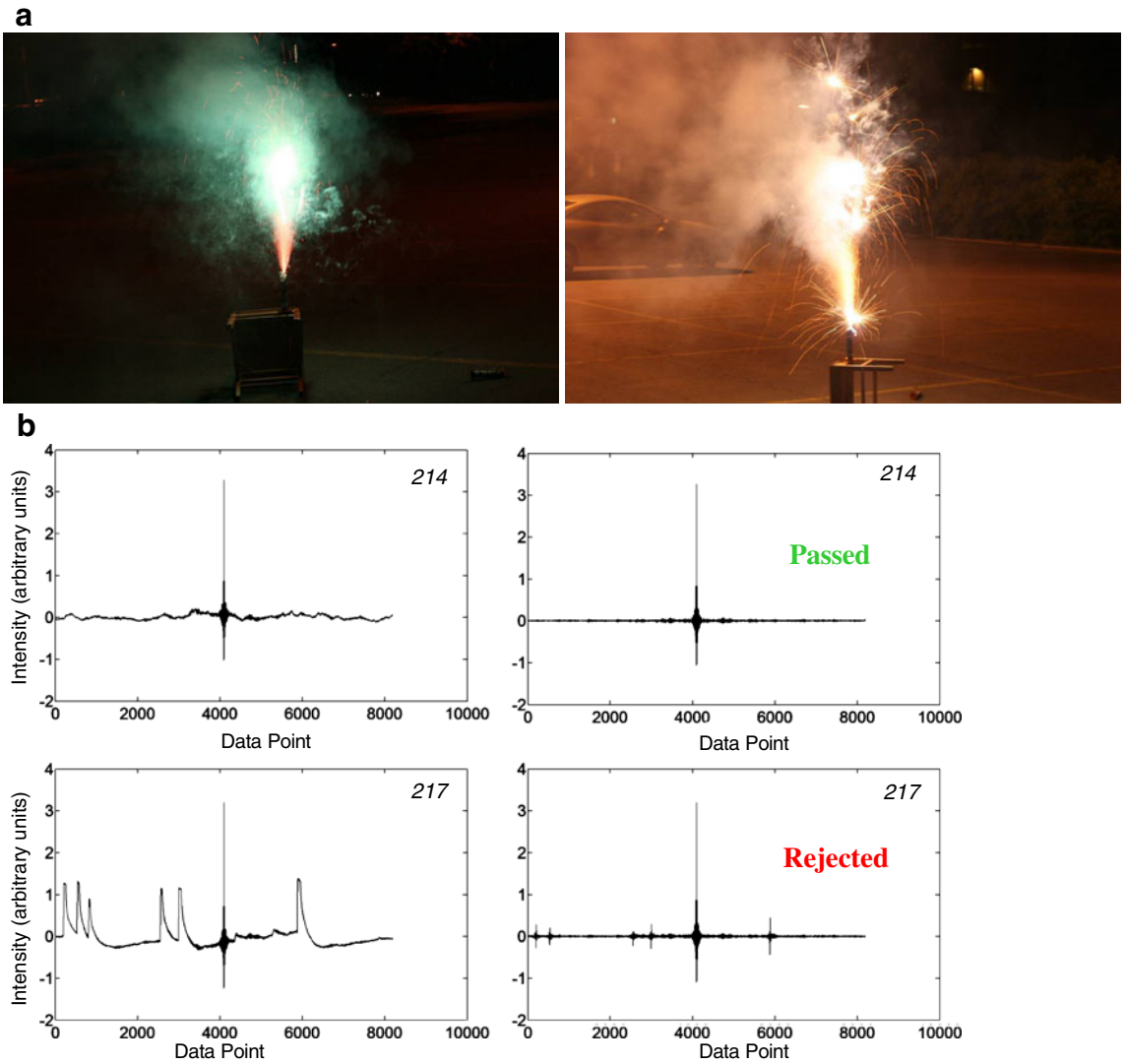

Fig. 5 **a** Firework during the acquisition of spectra 214 (*left*) and 217 (*right*). The spectrum produced a steady stream of smoke but towards the end changed to a "crackle". **b** Interferograms measured during ignition of the firework shown in **a** as measured (*left-hand side*) and after application of the high-pass filter (*right-hand side*). The interferograms measured during the early stages of ignition of this firework were passed by the rejection criterion while those measured during the "crackling" stage were rejected

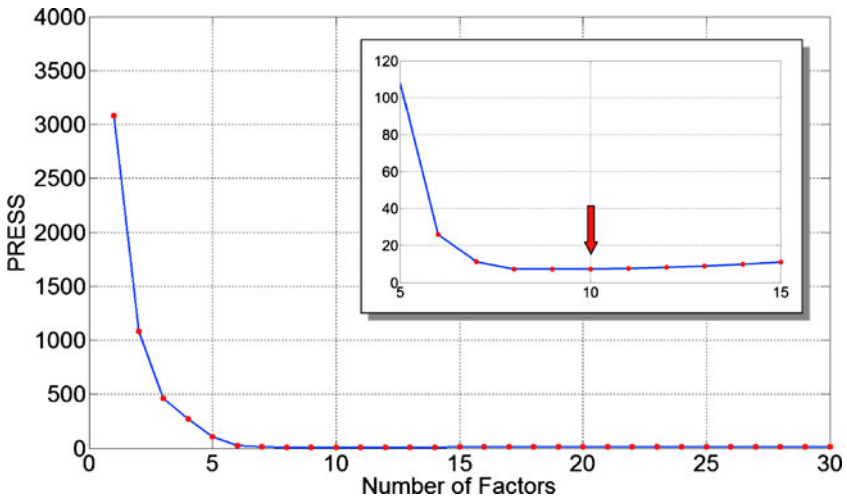

Fig. 6 Plot of PRESS against number of factors used in the PLS cross validation for calibration set #1; (*inset*) expanded region to this plot to show the minimum value of PRESS occurring for 10 factors

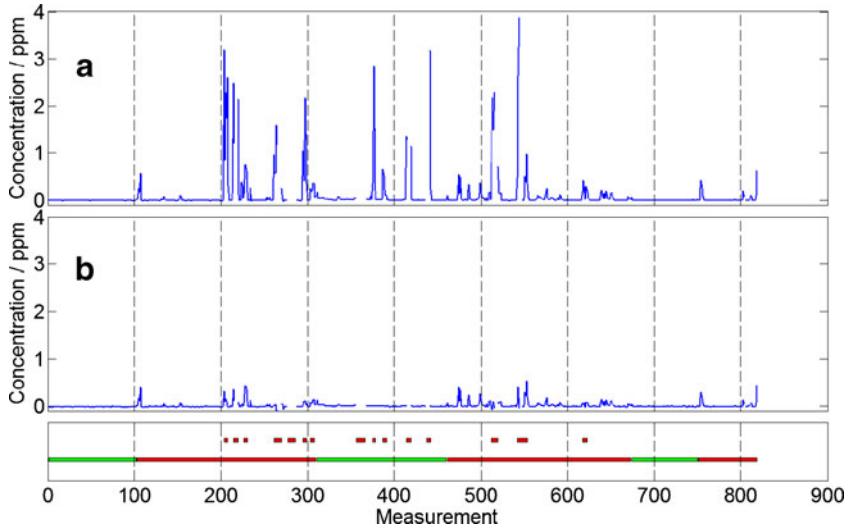

Fig. 7 Concentrations of diethyl ether in the 777 OP/FT-IR measurements processed by PLS using **a** Calibration Set #1 with ten factors and **b** Calibration Set #2 with 14 factors

one shown in Fig. 4a, produced a fairly constant shower of sparks. Even though the interferogram showed strong features due to the effect of the hot particles passing through the beam, they were all removed by the application of the high-pass filter, see Fig. 4b, and the filtered interferogram gave rise to an undistorted spectrum. Other fireworks were better described as producing a "crackle" that led to very high-frequency interference to the beam, in which case the interferograms were rejected. One of the fireworks started by emitting a steady green smoke but after a few seconds the nature of the emission changed to a "crackle", as shown in Fig. 5a. The distortion to the interferograms measured during the first part of this firework's emission was easily filtered out but the final interferogram had to be rejected, see Fig. 5b.

Partial least squares regression

The apparent concentration of diethyl ether in the beam was predicted through the application of PLS regression, using a set of calibration spectra that were synthesized from 54 single-beam background spectra that had been measured over a period of 9 months, at least 2 years before the spectra reported in this paper were acquired. These background spectra were measured in pristine air over pathlengths from 40 to 500 m under conditions such that the temperature and relative humidity of the atmosphere varied over as wide a range as possible. Each of these background spectra was corrected for the non-linear response of the MCT detector, ratioed against a short-pathlength background and converted to absorbance in the way described above [3]. In this way, we obtained a series of spectra of the atmosphere in which the absolute intensities of the lines in the rotation–vibration spectrum of water vapor varied greatly both because of the range of pathlengths covered (50–500 m) and the range in temperature when the spectra were measured (−5 °C to 35 °C). Because of this range in pathlength and temperature, both the absolute and relative intensities of the lines in the vibration–rotation spectrum of water vapor varied significantly. Furthermore, because the spectra were measured over total pathlengths as long as 500 m, the baseline of these spectra also showed considerable variation. A scaled reference spectrum of diethyl ether was added to each of these background spectra and the path-integrated concentration of the ether was calculated from the factor by which each spectrum was scaled. This set of spectra was used as Calibration Set #1 for the PLS regression.

The number of factors required for Calibration Set #1 was found by plotting the predicted residual error sum of squares (PRESS) against the number of factors used and it was found that ten factors were required, see Fig. 6. This is the same number that was found by Hart et al. when they first reported this approach [10, 11], so we are confident that this is a reasonable number. It can be seen that the last three factors only improved the result slightly but, because the ether concentration was so low, they were still found to be necessary to yield the most accurate predictions.

The result of calculating the concentration of diethyl ether using Calibration Set #1 for the 777 spectra that were retained after applying the rejection criterion is shown in Fig. 7a. It can be seen that *in the absence of fireworks*, even though the concentration of ether varies considerably because of the effect of wind gusts, its average concentration over the beam path never exceeds 1 ppm. To check the validity of the calibration set (which, as noted above, was measured 2 years before the spectra shown in Fig. 2), we augmented Calibration Set #1 with spectra 1 through 20 and then performed PLS on the remaining spectra. The resulting predictions changed only minimally. The validity of the results was verified by estimating the concentration of ether using Beer's Law for spectrum #105 (for which the

concentration of ether was known to be high as the Petri dish had been filled immediately beforehand). The path-integrated concentration was calculated as 13.3 ppm m, as compared to 14 ppm m obtained with Beer's law (see Fig. 3).

On the other hand, when fireworks are emitting hot oxide particles into the beam, the *calculated* concentration of ether is much higher than 1 ppm, see Fig. 7b. There is no reason for the ether concentration to show such a dramatic change, so these results are clearly in error. This result is caused by the lack of spectra in the calibration set that contain any information on the smoke particle spewing from the fireworks.

A new calibration set was constructed by augmenting Calibration Set #1 with 21 spectra that were measured in the presence of the fireworks but with no ether in the beam. These 21 spectra were #374–379 (firework #9), #386–392 (firework #10), #413–415, #419, and #420 (firework #11, *spectra #416–418 were rejected*), and #436, #441, and #442 (firework #12, *spectra #437–440 were rejected*). Although spectra #356–366 were also measured in the presence of a firework (firework #8) and without ether, all the 11 measurements were found to be invalid and rejected, and thus could not be used in this calibration set. Because the emissions for different fireworks varied, it was found that 15 factors were required to obtain a minimum in the PRESS plot. The concentrations of ether that were calculated using this calibration set (Calibration Set #2) are shown in Fig. 7b. In this case, the ether concentrations calculated when no fireworks were present are approximately the same as when the prediction was made using Calibration Set #1, but the concentrations calculated when the fireworks were emitting incandescent oxide particles into the beam were much more realistic.

We therefore conclude that by augmenting Calibration Set #1 with spectra that were measured when the effect of fireworks was observed but when ether was absent, the concentration of ether is correctly predicted. If this condition is not met, the calculated concentration of the analyte will be in error.

Target factor analysis

The main goal of the project was to find an optimal approach for detecting the first appearance of a chemical agent in the atmosphere under conditions of battlefield clutter. While PLS regression is usually an excellent approach for calculating the concentration of a target molecule in normal conditions, the requirement that the calibration set must represent all sources of variance in the prediction set cannot always be met, especially in the field of battle where the material emitted by an incoming missile is not known. An alternative technique for detecting the presence of a given compound under this circumstance is TFA [12]. In TFA, a principal component analysis is carried out on a data set and the presence of the target molecule is detected by rotating the eigenvectors in order to match one to the spectrum of the target molecule in a least squares manner. Thus, even when both the target molecule and other interferents appear at the same time (but with varying concentrations), it is possible that TFA will allow the detection of the target within a few seconds after its spectrum is measured with a sufficiently high signal-to-noise ratio. We have presented two detailed discussions of TFA and its application to OP/FT-IR spectroscopy [6, 13].

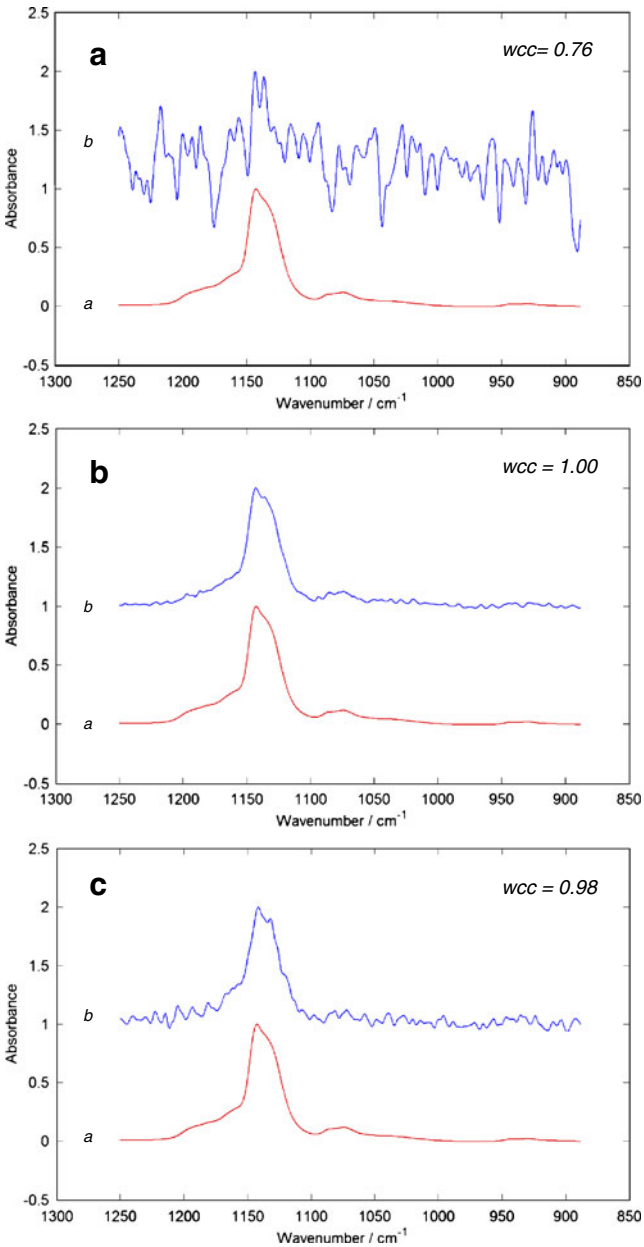

Fig. 8 Results of TFA for **a** spectra 1–100, **b** spectra 101–200, and **c** spectra 220–307 (*blue*). For comparison, the reference spectrum of diethyl ether is shown in *red* in each panel

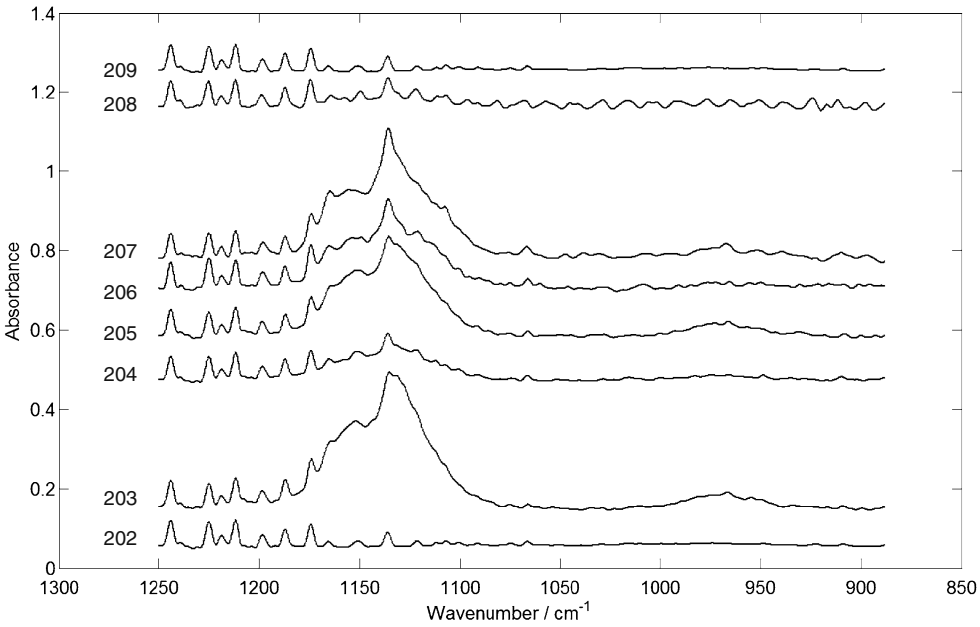

Fig. 9 Spectra measured while emissions from the first firework were streamed into the infrared beam. All interferograms were treated with a high-pass filter and the single-beam spectra were corrected for the non-linear response of the MCT detector. The spectra are offset for clarity

Recently, we demonstrated that a successful way of matching the result of TFA to the spectrum of the target molecule (diethyl ether in this case) even when the signal-to-noise ratio is low, is to calculate the weighted correlation coefficient (wcc) between the result of TFA and the reference spectrum of the target [14]. The weighted correlation coefficient is calculated in a similar way to the conventional correlation coefficient but larger weights are assigned to those wavelengths that have relatively high absorbance in the reference spectrum. In this work, the target molecule was originally deemed to be absent if wcc <0.90 and present if wcc >0.90 [14].

Typical results of target factor analysis of the first 307 spectra are shown in Fig. 8, along with the wcc value in each case. The first two results, obtained in the absence of fireworks, are not surprising as ether is clearly shown to be absent for spectra 1–100 (wcc=0.76) and present for spectra 101–200 (wcc=1.00), see Fig. 8a and b, respectively. Even when the emissions from fireworks were passed into the infrared beam, the presence of ether in the beam was definitively shown (wcc=0.99). In other words, the TFA algorithm was clearly able to recognize the presence of ether in the beam even when hot oxide particles, which had strong absorption in the same spectral region as the strong band of ether caused a large-enough interference as to cause PLS to give an incorrect result unless the calibration set included spectral data from each of the different fireworks.

One example of the type of interference that was created by the fireworks will be given. The firework that was burning between spectra 202–209 had two distinct phases: colored smoke was emitted in the first phase, followed by a shower of sparks (see Fig. 4a) in the second phase (note that none of these spectra was rejected). The spectra measured during this

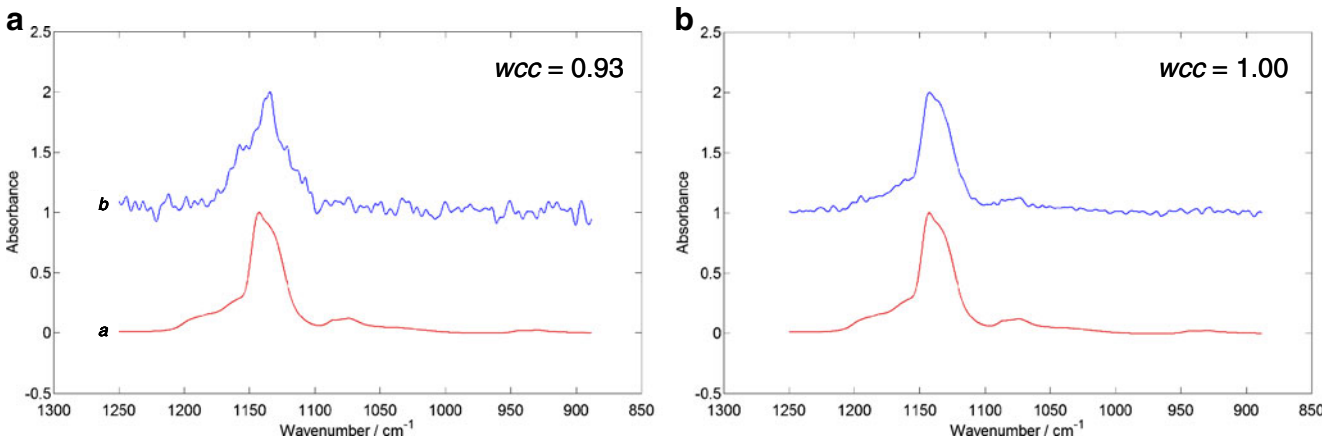

Fig. 10 **a** The result of TFA for spectra 356–442, when no ether was present in the beam but the emissions from several fireworks were streamed into the infrared beam. **b** The result of TFA for spectra 512–622 when ether was known to be in the beam and three fireworks were set off at different times

time are shown in Fig. 9. The broad overlapping bands that are seen in the atmospheric window are caused by absorption by very small particulate matter. The fact that these bands are not distorted by the Christiansen effect indicates that their particle size is much smaller than the wavelength [15], so that Beer's law is probably obeyed and the spectra are amenable to principal components analysis. The profile of these bands changes as the chemical nature of the emitted material changes from the first to the second phase. In spite of the maxima of these bands being found at a very similar wavenumber to the maximum of the bands in the spectrum of diethyl ether, the value of the weighted correlation coefficient was very close to unity.

All the results were not quite so straightforward, as sometimes the accuracy of the results (i.e., the value of wcc) appeared to depend on the variation of the spectra of the fireworks. For example, when TFA was performed on spectra 356–442, for which ether was absent but several fireworks were set off, a wcc value of 0.93 was obtained (see Fig. 10a). This value would give rise to a false-positive identification using the criterion that wcc should be greater than 0.90, even though an experienced spectroscopist would probably recognize the difference between this result and the reference spectrum of diethyl ether. Conversely, for spectra 512–622 when ether was present in the beam and some fireworks were set off, an excellent match was found, as shown in Fig. 10b. The spectra of the emissions from the three fireworks were quite similar, which allowed them to contribute to just one or two eigenvectors calculated during PCA. From these results, it is logical to conclude that TFA works most successfully when the spectrum of all possible interferents is significantly different from the spectrum of the target and suggests that our previous acceptance criterion of wcc >0.90 should be changed to wcc >0.95.

In summary, we have shown that TFA can be used to signal the presence of a given target analyte under conditions of background clutter where the application of PLS regression can give false-positive results.

Acknowledgment This work was funded by contract W91ZLK08P0739 from the Edgewood Chemical Biological Center, Edgewood Arsenal, US Army and by National Natural Science Foundation in China (Grant No. 20705032).

References

1. Russwurm GM, Childers JW (2002) Open-path Fourier transform spectroscopy. In: Chalmers JM, Griffiths PR (eds) Handbook of vibrational spectroscopy, Vol. 2. Wiley, Chichester, pp 1750–1773
2. Griffiths PR, de Haseth JA (2007) Chapter 22 in Fourier transform infrared spectrometry, 2nd edn. Wiley, Hoboken, pp 463–479
3. Griffiths PR, Shao L, Leytem AB (2009) Anal Bioanal Chem 393:45–51
4. European Standard EN 15483 (2008) Ambient air quality—atmospheric measurements near ground with FTIR spectroscopy. European Committee for Standardization, Brussels
5. Sharpe SW, Johnson TJ, Chu PM, Kleimeyer J, Rowland B (2003) Proc SPIE 5085:19–27
6. Shao L, Griffiths PR (2007) Anal Chem 79:2118–2124
7. Shao L, Pollard MJ, Griffiths PR, Westermann DT, Bjorneberg DL (2007) Vib Spectrosc 43:78–85
8. Richardson RL, Griffiths PR (1997) Appl Spectrosc 51:1254–1255
9. Shao L, Griffiths PR (2008) Anal Chem 80:5219–5224
10. Hart BK, Griffiths PR (1998) Proc 11th Int Conf Fourier Transform Spectrosc, Am Inst Phys Conf Procedings 430: 241
11. Hart BK, Berry RJ, Griffiths PR (2000) Environ Sci Technol 34:1346–1351
12. Malinowski ER (2002) Factor analysis in chemistry, 3rd edn. Wiley, New York
13. Shao L, Griffiths PR (2010) Anal Chem 82:106–114
14. Griffiths PR, Shao L (2009) Appl Spectrosc 63:916–919
15. Pollard MJ, Griffiths PR, Nishikida K (2007) Appl Spectrosc 61:860–866